DOI 10.1007/s10812-021-01146-y
Journal of Applied Spectroscopy, Vol. 88, No. 1, March, 2021 (Russian Original Vol. 88, No. 1, January–February, 2021)

ISOLATION AND IDENTIFICATION OF 9-*cis* ASTAXANTHIN BY HPLC, FT-IR, AND NMR SPECTRA

Y. Wang,[a] Y. Wu,[b] T. Wang,[a] and D. Qiu[a,b,*]

UDC 539.143.43

This study aims to perform a detailed qualitative analysis of astaxanthin isomers. A rapid, open column chromatography method was developed to separate astaxanthin geometrical isomers in gram-scale levels. Chromatographic separation was performed using two silica gel columns with dichloromethane/n-hexane/diethyl ether (2:1:1, v/v/v) as elution system. The isolated isomers were identified as all-trans, 9-cis, 13-cis, and 15-cis astaxanthin, according to previously reported C_{30} high-performance liquid chromatography (HPLC) analysis data. Further, the fine structure of the single 9-cis astaxanthin isomer, as well as all-trans astaxanthin, was determined successfully for the first time by Fourier-transform infrared spectroscopy (FT-IR), one-dimensional ^{1}H and ^{13}C nuclear magnetic resonance (NMR) spectroscopy, and two-dimensional homonuclear correlation and heteronuclear correlation NMR spectroscopy.

Keywords: *astaxanthin, isolation, identification, isomer, nuclear magnetic resonance spectra.*

Introduction. Astaxanthin (3,3′-dihydroxy-β,β′-carotene-4,4′-dione), a naturally occurring carotenoid produced by the microalgae *Haematococcus pluvialis* and yeast such as *Phaffia rhodozyma* and *Xanthophyllomyces dendrorhous* [1], has attracted considerable attention due to its economic value as a pigment in the aquaculture and food industries [2]. These carotenoids are also known to possess strong antioxidant properties [3–5]. In recent years, numerous studies have reported that astaxanthin has potential health-enhancing effects in the prevention and treatment of various diseases, such as cancer [6–8], cardiovascular [9, 10], and neurological disorders [11].

Due to the increase in demand for astaxanthin in food, cosmetics, medicine, and other healthcare industries, along with natural astaxanthin, synthetic astaxanthin also plays an essential role in the commercial market, even though it raises some food safety concerns. The double bonds of the astaxanthin polyene chain can exist in the *cis* or *trans* configurations, also designated as *E*/*Z* conformations. *Cis* isomers have always been observed at positions 9 and 13, and due to their unhindered configuration, these geometrical isomers exhibit different antioxidant activities [12] and bioavailability [13] when compared to all-*trans* astaxanthin (Scheme 1).

Many researchers have demonstrated that temperature, solvent [14, 15], light, acid [16, 17], and ions [18, 19] could cause isomerization or degradation of astaxanthin products, and reduce their quality. Therefore, the separation and identification of *cis*/*trans* isomers are crucial for studying the chemical properties and safety of astaxanthin. With the development of high-performance liquid chromatography (HPLC), common astaxanthin isomers have been separated well using a normal-phase silica column (Si_{60}) [20]. In our previous studies, a C_{30} and Si_{60} HPLC system was established to successfully isolate 11 geometrical isomers and four epoxides of astaxanthin [21, 22]. Though preparative Si_{60} and C_{30}-HPLC isolated *trans/cis* astaxanthin and its diacetates, these technologies are somewhat difficult for gram-scale preparation because of the high cost and low yield. To the best of our knowledge, no information on separation and purification of a single *cis* astaxanthin isomer in gram-scale levels has been reported.

High-performance liquid chromatography–atmospheric pressure chemical ionization–mass spectrometry (HPLC–APCI–MS) and Fourier transform infrared spectroscopy (FT-IR) were commonly used in the determination of astaxanthin

*To whom correspondence should be addressed.

[a]School of Materials and Chemical Engineering at Ningbo University of Technology, Ningbo 315211, China; email: wangyajuan@nbut.edu.cn; [b]Zhejiang NVB Co. Ltd., High-Tech Industry Zone, XinChang 312500, China. Published in Zhurnal Prikladnoi Spektroskopii, Vol. 88, No.1, pp. 109–118, January–February, 2021. Original article submitted January 3, 2020.

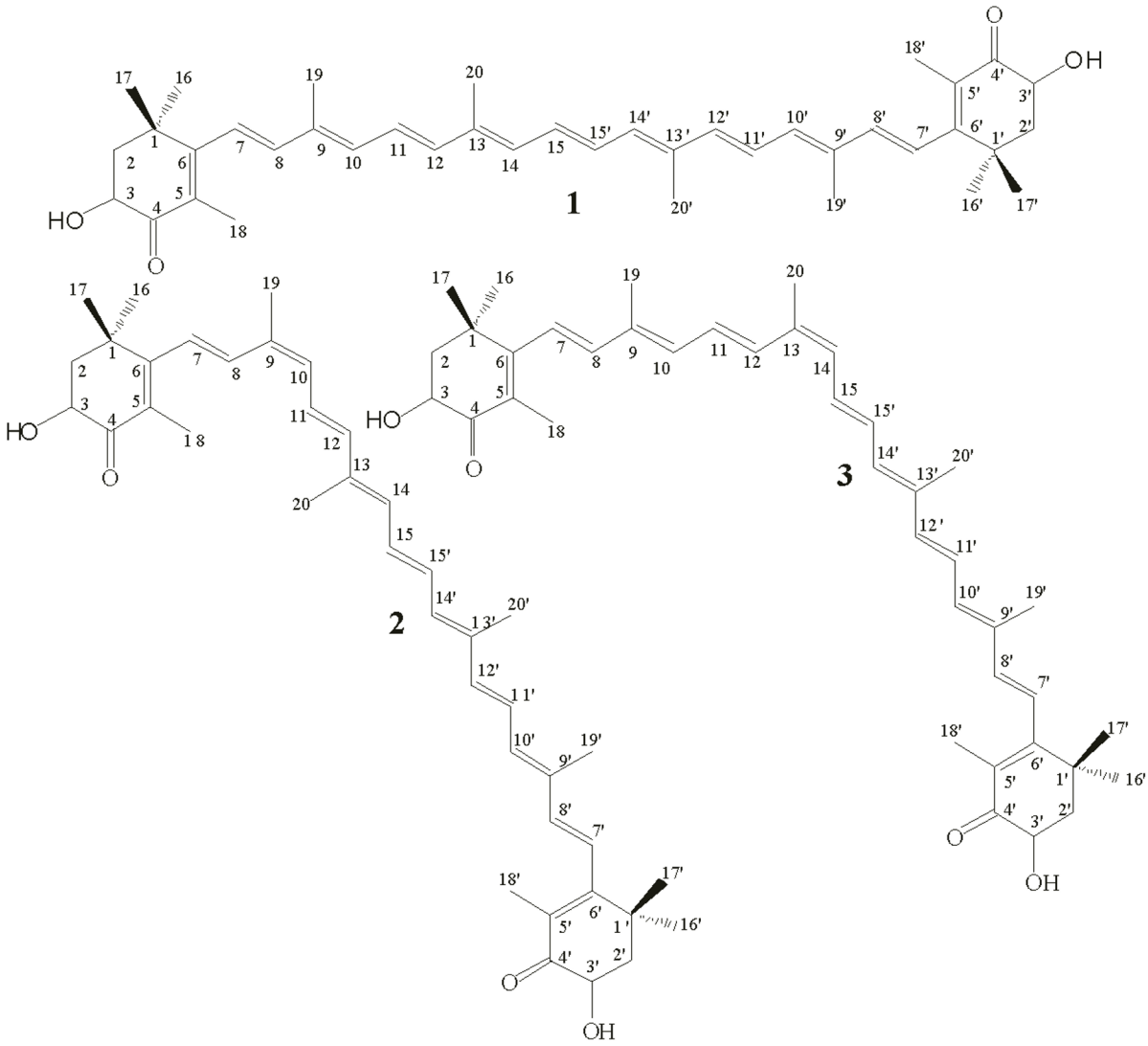

Sheme 1. Geometrical isomers of astaxanthin: (1) all-*trans* astaxanthin; (2) 9-*cis* astaxanthin; (3) 13-*cis* astaxanthin

isomers, astaxanthin esters, and polysaccharide derivatives [23–25]. In addition, all-*trans*, 9-*cis,* and 13-*cis* astaxanthin were unambiguously assigned by ^{1}H, ^{1}H–^{1}H correlation spectroscopy (COSY) and microcoil nuclear magnetic resonance (NMR) spectroscopy [26], while impurities of all-*trans* astaxanthin were isolated and analyzed by ^{1}H and ^{13}C NMR [27, 28]. It is also worth mentioning that isomers of astaxanthin diacetate were isolated by home-made Si_{60} HPLC and identified by ^{1}H NMR [20]. Compared to the all-*trans* isomer, spectroscopic information on a single high-purity *cis* astaxanthin isomer is not abundant.

We believe that the lack of knowledge on *cis* astaxanthin is partly because of the limitations on its purity. If the *cis* isomer can be separated and prepared rather than isolated by semi-preparative HPLC, accurate identification and quantification would be possible, which would benefit further research on astaxanthin. We reported the isomerization of synthetic all-*trans* astaxanthin by thermal treatment and isolation of astaxanthin isomers using a rapid, open column chromatography (OCC) method. Then the purities of the isolated samples were identified by high-performance liquid chromatography (HPLC) analysis. Further, with great interest, we not only verified the purity but also focused on authentically elucidating the structure of 9-*cis* astaxanthin compared to that of all-*trans* by FT-IR and NMR spectra.

Experimental. Synthetic astaxanthin crystal in the all-*trans* isomer form (for ^{1}H NMR and ^{13}C NMR of the chemical, see Fig. 1) was supplied by Zhejiang NVB Co. Ltd. (Xinchang, Zhejiang, China). HPLC grade hexane and methanol were purchased from Shield Co. Ltd. (Tianjin, China), and methyl tert-butyl ether (MTBE) was purchased from Tedia Company (USA). Deuterated chloroform ($CDCl_3$) with 0.03% tetramethylsilane (TMS) was purchased from Aldrich.

Other chemicals were of analytical grade and commercially available and used directly without further purification unless otherwise stated.

Preparation of astaxanthin isomers by OCC. Synthetic astaxanthin crystal was refined and recognized as all-*trans* astaxanthin (sample a). Crystallized astaxanthin (1.0 g) was dissolved in chloroform (500 mL) by heating the solution at 50°C in the dark for 24 h. The solution was then directly applied to two silica gel columns (120 × 8.0 cm i.d.). The columns were eluted employing a mixture of dichloromethane, *n*-hexane, and diethyl ether (2:1:1; v/v/v). In order to reduce the risk of side-reactions promoted by the adsorbent and eluent, the column elution was stopped once all bands were distributed entirely, and the silica gels were slowly extruded to the salvers using nitrogen. Three bands were identified using thin-layer chromatography (TLC). The main portion of each band containing the same component except for that of all-*trans* was cut out carefully, mixed, extracted by dichloromethane quickly, and dried by vacuum evaporation at 20°C. Then the samples were dissolved by cyclohexane and freeze-dried to yield two isolated astaxanthin samples (samples b and c).

For TLC detection a few silica gel bands were collected, dissolved in dichloromethane, and loaded to the marked point about 7 mm from the bottom of the silica gel plate (25 × 75 mm; layer thickness 0.1 mm). The plates were developed in dichloromethane/*n*-hexane/diethyl ether (2:1:1; v/v/v), and the sample spots on the chromatogram were detected by the naked eye. The recording was done using a digital camera (OLYMPUS SP-550UZ).

The HPLC analysis of all the samples (samples a, b, and c) was carried out according to our previous method [21]. The samples (20.00 mg, dry weight) were dissolved in 10 mL of THF, and 50 μL of this solution was collected and diluted with 2 mL of each mobile phase before injecting (20 μL) into the system.

The FT-IR spectra were collected with 2.0 mg all-*trans* or 9-*cis* astaxanthin sample in KBr pellets using a Tensor 27 spectrometer (Bruker Optik GmbH, Ettlingen, Germany) with an RT-DLa TSG internal detector having a resolution of 4 cm^{-1} in the region 400–4000 cm^{-1}.

All NMR spectra were recorded on the Bruker (Germany) Avance III spectrometer operating at 600 MHz for ^{1}H and 125 MHz for ^{13}C. About 10 mg and 100 mg of astaxanthin samples were dissolved in 0.5 mL $CDCl_3$ for ^{1}H and ^{13}C analysis, respectively. ^{1}H NMR, ^{13}C NMR, and two-dimensional NMR spectra were all obtained at room temperature (25°C) using TMS as the internal standard. All chemical shifts are measured on the δ-scale in parts per million (ppm). The chemical shift scales are internally compared to the solvent residual peak of cyclohexane at 1.43 and 26.94 ppm in $CDCl_3$ for ^{1}H and ^{13}C, respectively. Data analysis was performed with MestReNova 6.1.1 NMR software.

Results and Discussion. *OCC separation and HPLC analysis of astaxanthin isomers.* TLC was developed to determine the main isomers of astaxanthin solution tentatively, and the three spots obtained. Based on the TLC result, three astaxanthin isomers (distinguished as samples a, b, and c, respectively) were obtainned by OCC separation. In our previous work, the analysis of the astaxanthin sample by C_{30} and Si_{60}-HPLC method was compared and studied, and the peaks of C_{30}-HPLC were further identified by HPLC–DAD and HPLC–APCI–MS [22]. Since the HPLC conditions were similar to the reported systems, the identification results could be extrapolated to this study. According to the chromatographic retention behavior of astaxanthin isomers, the peaks 1–4 of C_{30}-HPLC in Fig. 2a were identified as all-*trans*, 9-*cis*, 13-*cis*, and 15-*cis* astaxanthin with retention times of 21.41, 32.68, 18.44, and 16.58 min, respectively.

Interestingly, samples a and b generated only one peak each in both the HPLC systems, while sample c generated two peaks (peaks 3 and 4) by C_{30}-HPLC (Fig. 2a) and one peak (peak 3) by Si_{60}-HPLC (Fig. 2b). Peaks 1–3 of Si_{60}-HPLC were recognized as all-*trans*, 9-*cis*, and 13-*cis* astaxanthin; however, the comparison of the separation of sample c (isolated by OCC and collected from one band) by two HPLC conditions showed that 13-*cis* and 15-*cis* astaxanthin could not be separated in Si_{60}-HPLC (and also the OCC system), suggesting that our C_{30}-HPLC method was more useful for analysis of astaxanthin isomers. Therefore, samples a and b (identified as all-*trans* and 9-*cis* astaxanthin, respectively) were chosen for further studies to elucidate their structures as well as purities in detail by FT-IR and NMR spectroscopy. We did not focus on the mixture of 13 and 15-*cis* astaxanthin obtained during the separation process in the following structure determination studies.

FT-IR spectra of all-trans and 9-cis astaxanthin. The 400 to 4000 cm^{-1} region of all-*trans* astaxanthin's IR spectrum (Fig. 3a) offered several key pieces of information about chemical bonds and functional groups as follow: 974 cm^{-1} (s), ν_{trans} =CH, C =C; 1032 cm^{-1} (m), 1071 cm^{-1} (m), ν C–O; 1280 cm^{-1} (m), *ν* C–O, β OH; 1364 cm^{-1} (m), δ_s CH_3; 1455 cm^{-1} (w), δ_{as} CH_3; 1550 cm^{-1} (s), *ν* C =C; 1649 cm^{-1} (vs), ν C =O, conjugated; 2862 cm^{-1} (w), ν_s CH_2, ν_s CH_3; 2921 cm^{-1} (m), ν_{as} CH_2; 2970 cm^{-1} (m), ν_{as} CH_3; 3032 cm^{-1} (w), ν (=CH); 3494 cm^{-1} (w), ν OH. The spectrum showed good agreement with our previous report on all-*trans* astaxanthin [25]. When compared with the spectrum of all-*trans* astaxanthin, no new

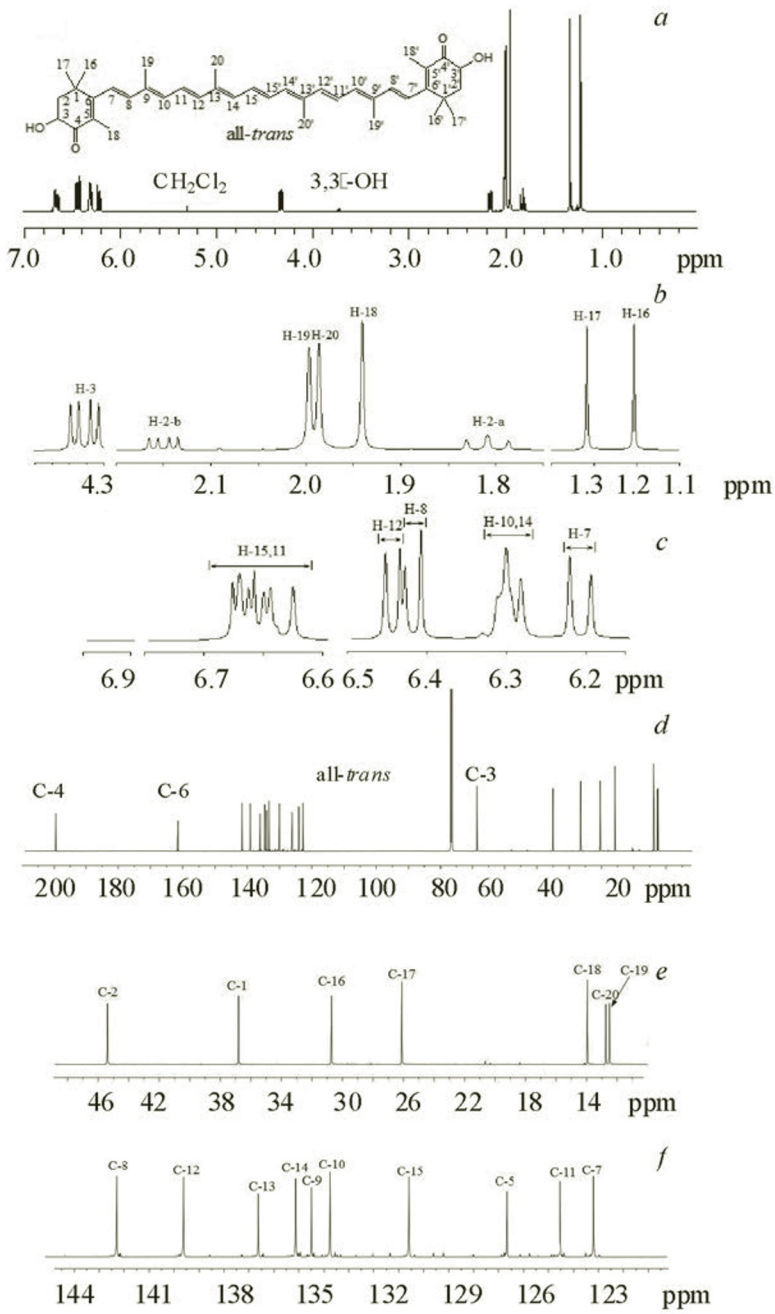

Fig. 1. ^{1}H NMR (a–c) and ^{13}C NMR (d–f) spectra of all-*trans* in $CDCl_3$. Structures of all-*trans* astaxanthin are inserted and assignments for protons are listed on the top of the corresponding resonances. The regions 7–0 (a), 4.38–4.3, 2.2–1.75, 1.4–1.1 (b), 7–6.9, 6.75–6.6, 6.5–6.15 (c), 210–0 (d), 48–12 (e), and 145–120 ppm (f). Each labeled number represents all of the symmetric carbons.

bands and groups were found in Fig. 3b, suggesting that the separated sample b was still an astaxanthin molecule rather than an epoxide or other byproducts. It can be observed that there was an obvious shift in some bands due to the effects of isomerization: 961 cm^{-1} (s), ν_{trans} (=CH), C =C, shift –13 cm^{-1}; 1558 cm^{-1} (s), *ν* C =C, shift +8 cm^{-1}; 1658 cm^{-1} (vs), ν C =O, conjugated, shift +9 cm^{-1}; 2961 cm^{-1} (m), ν_{as} CH_3, shift –9 cm^{-1}; 3468 cm^{-1} (w), ν OH, shift –26 cm^{-1}.

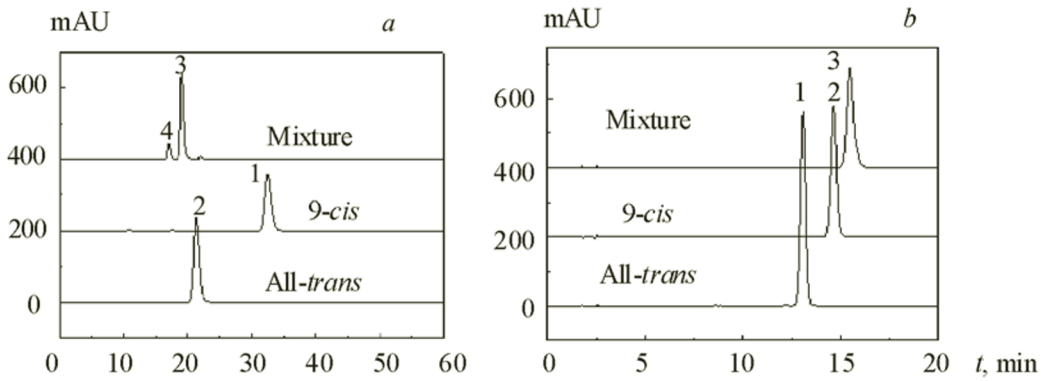

Fig. 2. C_{30}-HPLC (a) and Si_{60}-HPLC (b) chromatograms of all-*trans*, 9-*cis* astaxanthin, as well as 13-*cis* and 15-*cis* astaxanthin mixture, isolated by OCC.

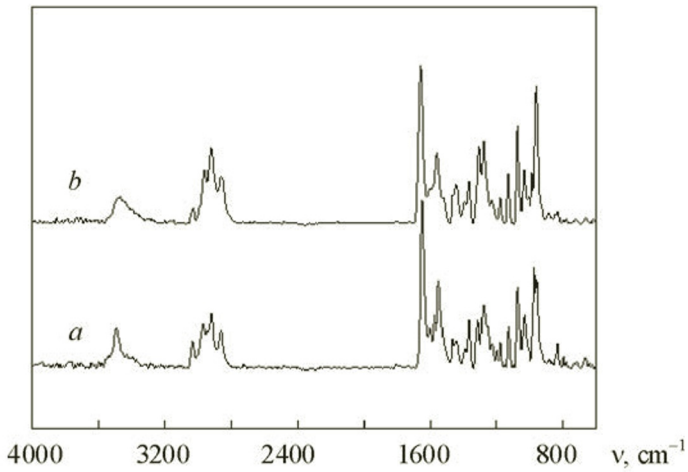

Fig. 3. FT-IR spectra of all-*trans* (a) and 9-*cis* astaxanthin (b)

Complete assignments of ^{1}H NMR spectra of 9-cis astaxanthin. To the best of our knowledge, the complete ^{1}H NMR signal assignments for 9-*cis* astaxanthin have not yet been made. Grynbaum [23] and Holtin [26] used ^{1}H and ^{1}H–^{1}H COSY NMR to identify the protons in the olefinic portion, but not the alkyl region. In the reported literature, deuterated acetone was chosen as the solvent rather than the more conventional deuterated chloroform. Furthermore, the research on 9-*cis* astaxanthin diacetate served as a support system for the assignment of the signals of 9-*cis* astaxanthin [20].

The full ^{1}H NMR spectrum and its local amplification of 9-*cis* astaxanthin in $CDCl_3$ are shown in Fig. 4. Apart from the peaks of residual solvents dichloromethane/*n*-hexane, no other impurity peaks have been detected, which proves that the separation and analysis methods of OCC and HPLC are effective, and the purities of the isomers could be guaranteed. One of the most significant differences between these isomers is that the alkyl protons of 9-*cis* astaxanthin, such as H-18/18′, are separated while the ones of all-*trans* are not, and this rearrangement of 9-*cis* results in a non-centrosymmetric structure, abolishing the chemical equivalence of protons. Previous studies have found that the formation of a *cis* bond leads to a characteristic shift difference in the olefinic portion of carotenoids compared to the all-*trans* compound [29]. The isomeric shift difference ($\Delta\delta = \delta_{cis} - \delta_{trans}$) was found to make the variation between proton or carbon signals more intuitive. The chemical shifts (δ_H), isomeric shift differences ($\Delta\delta_H$), integrals (*I*), and assignments of 9-*cis* astaxanthin are listed in Table 1. The H-8 chemical shifts of 9-*cis* were strongly affected by a $\Delta\delta_H$ value of 0.538 ppm due to the newly formed *cis* bond at C-9 position as compared with all-*trans* astaxanthin. Meanwhile, H-10, H-11, and H-12 shift to a higher or lower field with $\Delta\delta_H$ values of –0.062, 0.05, and –0.085 ppm, respectively; however, others far from the *cis* bond show little change.

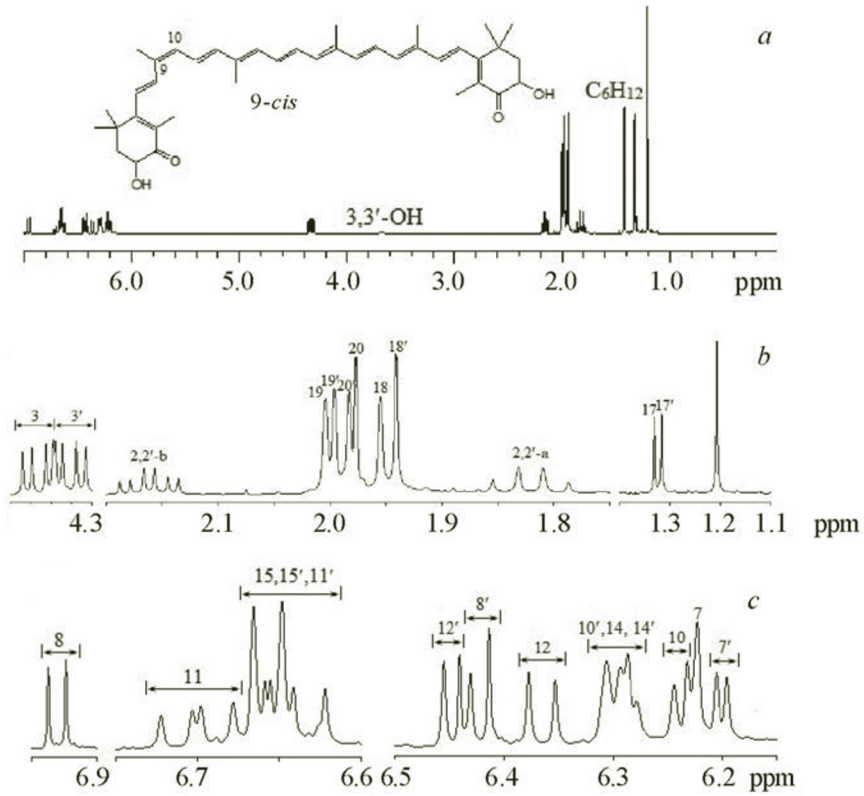

Fig. 4. ^{1}H NMR spectra of 9-*cis* astaxanthin in $CDCl_3$ in regions 7–0 (a); 4.38–4.3, 2.2–1.75, 1.4–1.1 ppm (b); 7–6.9, 6.75–6.6, 6.5–6.15 ppm (c). Each labeled number represents all symmetric protons.

Complete assignments of ^{13}C NMR spectra of 9-cis astaxanthin. The full ^{13}C NMR spectra of 9-*cis* astaxanthin in $CDCl_3$ are displayed in Fig. 5. As is widely known, all carbon signals, whether they are attached to protons or not, can be shown in the interval of 100–150 ppm for organic molecules. Almost every nonequivalent carbon exhibits a single peak in ^{13}C NMR [30, 31], which offers further information to make the identification results of the geometrical isomers more trustworthy. Based on the above discussions of ^{1}H NMR, the procedure of the ^{13}C NMR assignment turned out to be relatively simple. All chemical shifts (δ_C), isomeric shift differences ($\Delta\delta_C$), and assignments of 9-*cis* astaxanthin are summarized in Table 2.

The *cis* bond built at C-9 position for 9-*cis* astaxanthin affects the directly attached carbons the most. The carbons C-8 (134.14 ppm) and C-10 (132.79 ppm) are shifted to a higher field with $\Delta\delta_C$ values of –8.15 ppm (C-8) and –2.28 ppm (C-10), while C-19/19 (20.36 ppm) is shifted to a lower field with a $\Delta\delta_C$ value of 7.77 ppm. All-*trans* and 9-*cis* astaxanthin can be distinguished from each other through these features. Moreover, the olefinic or alkyl carbons in the vicinity also suffer different influences. The olefinic $\Delta\delta_C$ values of C-7, C-11, and C-12 are 1.62, –1.48, and 1.05 ppm, while the alkyl $\Delta\delta_C$ values of C-20 and C-18 are –0.24 and 0.20 ppm, respectively. Similar to the chemical shifts of protons, the shifts of carbons away from the *cis* bond are almost unchanged.

^{1}H–^{1}H COSY and ^{1}H–^{13}C HSQC spectra of all-trans and 9-cis astaxanthin. While some signals in the olefinic region of one-dimensional NMR spectra could not be unambiguously assigned since the spectrum peaks strongly overlapped, two-dimensional NMR spectra provide further information about the homonuclear and heteronuclear correlations (Fig. 6).

In the ^{1}H–^{1}H COSY spectrum of all-*trans* astaxanthin, H-3 proton is coupled with H-2a and H-2b, whereas H-2a and H-2b are coupled with each other. It is observed that H-2a and H-2b are adjacent to H-3. Moreover, olefinic proton H-11 is coupled with both H-10 and H-12 protons, but H-10 and H-12 are not coupled to each other, indicating that H-11 is placed in between H-10 and H-12. The other olefinic proton pairs are H-7 with H-8 and H-14 with H-15. Analogically, the

TABLE 1. Chemical Shifts (δ_H, ppm), Chemical Shift Differences ($\Delta\delta_H$, ppm), and Integrals (*I*) for Protons of 9-*cis* Astaxanthin

Position[a]	δ_H		$\Delta\delta_H$ [c]	*I*	
	Found	Reported[b]		Found	Theoretical
16 16′	1.207(s)	1.230	–	1.00	1.00
17	1.331(s)	1.350	0.014	0.48	0.50
17′	1.317(s)		–	0.50	0.50
18	1.955(s)	1.939	0.014	0.49	0.50
18′	1.940(s)	1.904	–0.001	0.52	0.50
20	1.978(s)	1.974	–0.009	0.47	0.50
20′	1.983(s)	1.990	–0.004	0.48	0.50
19	2.004(s)	2.003	0.006	0.47	0.50
19′	1.996(s)	2.003	–0.002	0.48	0.50
2,2′-a	1.820(m)	2.08–2.10	0.011	0.40	0.67
2,2′-b	2.161(m)		0.004	0.29	
3	4.350(m)	5.55	0.029	0.16	0.33
3′	4.321(m)	5.53	–	0.17	
7	6.223(s)	6.22	0.013	0.17	0.17
7′	6.200(d)	6.20	–0.010	0.17	0.17
14 14′ 10′	6.26–6.32(m)	6.30	–	0.47	0.50
10	6.238(d)	6.24	–0.062	0.18	0.17
8	6.960(d)	6.95	0.538	0.14	0.17
8′	6.422(d)	6.41	–	0.17	0.17
12	6.363(d)	6.36	–0.085	0.15	0.17
12′	6.448(d)	6.45	–	0.14	0.17
11	6.67–6.73(m)	6.71	~0.05	0.14	0.17
11′	6.60–6.67(m)	6.65	–	0.46	0.50
15 15′		6.67			

[a]See structures for atom numbering.

[b]Chemical shift of astaxanthin diacetate in $CDCl_3$ are from [20] and included here for comparison.

[c]Relative to the chemical shift of proton signal (δ_H) of all-*trans* astaxanthin.

recorded ^{1}H-^{1}H COSY spectrum of 9-*cis* astaxanthin offers more proton correlated peaks such as H-7′/H-8′ due to the non-centrosymmetric structure. The data described in ^{1}H-^{1}H COSY were consistent with the elucidated structures of all-*trans* and 9-*cis* astaxanthin by ^{1}H NMR. It is worth mentioning that the chemical shifts of H-10/11, H-14/14′ and H-15/15′ overlap so much that it is hard to distinguish them from each other, hence analysis of heteronuclear singular quantum correlation

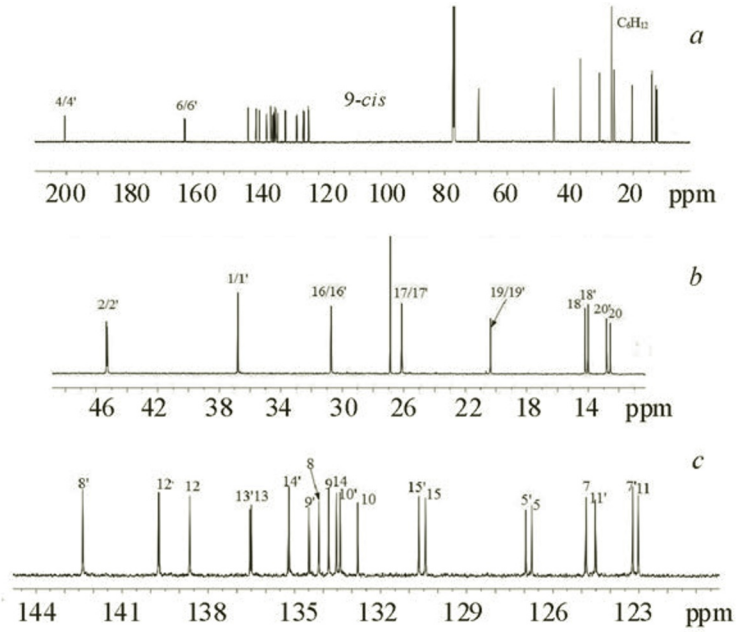

Fig. 5. ^{13}C NMR spectra of 9-*cis* astaxanthin in $CDCl_3$ in the regions 210–0 (a), 48–12 (b), and 145–120 ppm (c).

TABLE 2. C^{13} Chemical Shifts (δ_C, ppm) and Chemical Shift Differences ($\Delta\delta_C$, ppm) for Carbons of 9-*cis* Astaxanthin

Position[a]	δ_C	$\Delta\delta_C$ [b]	Position[a]	δ_C	$\Delta\delta_C$ [b]
19	20.36	7.77	5	126.73	–0.08
19′			5′	126.94	0.13
20	12.57	–0.24	15	130.43	–0.22
20′	12.81	0	15′	130.66	0.01
18	14.21	0.2	10	132.79	–2.28
18′	14.01	0	10′	133.4	–1.67
17	26.12	–0.01	14	133.53	–0.28
17′			9	133.81	–0.75
16	30.71	–0.01	8	134.14	–8.15
16′			9′	134.49	–0.07
1	36.77	0	14′	135.19	1.38
1′			13	136.52	–0.17
2	45.31	–0.07	13′		
2′			12	138.64	–1.05
3	69.19	–0.03	12′	139.72	0.03
3′			8′	142.37	0.08
11	123.03	–1.48	6	162.24	–0.04
7′	123.22	–0.01	6′	162.53	0.25
11′	124.51	0	4	200.45	0.01
7	124.85	1.62	4′		

[a]See structures for atom numbering.

[b]Relative to the chemical shift of carbon signal ($\Delta\delta_C$) of all-*trans* astaxanthin.

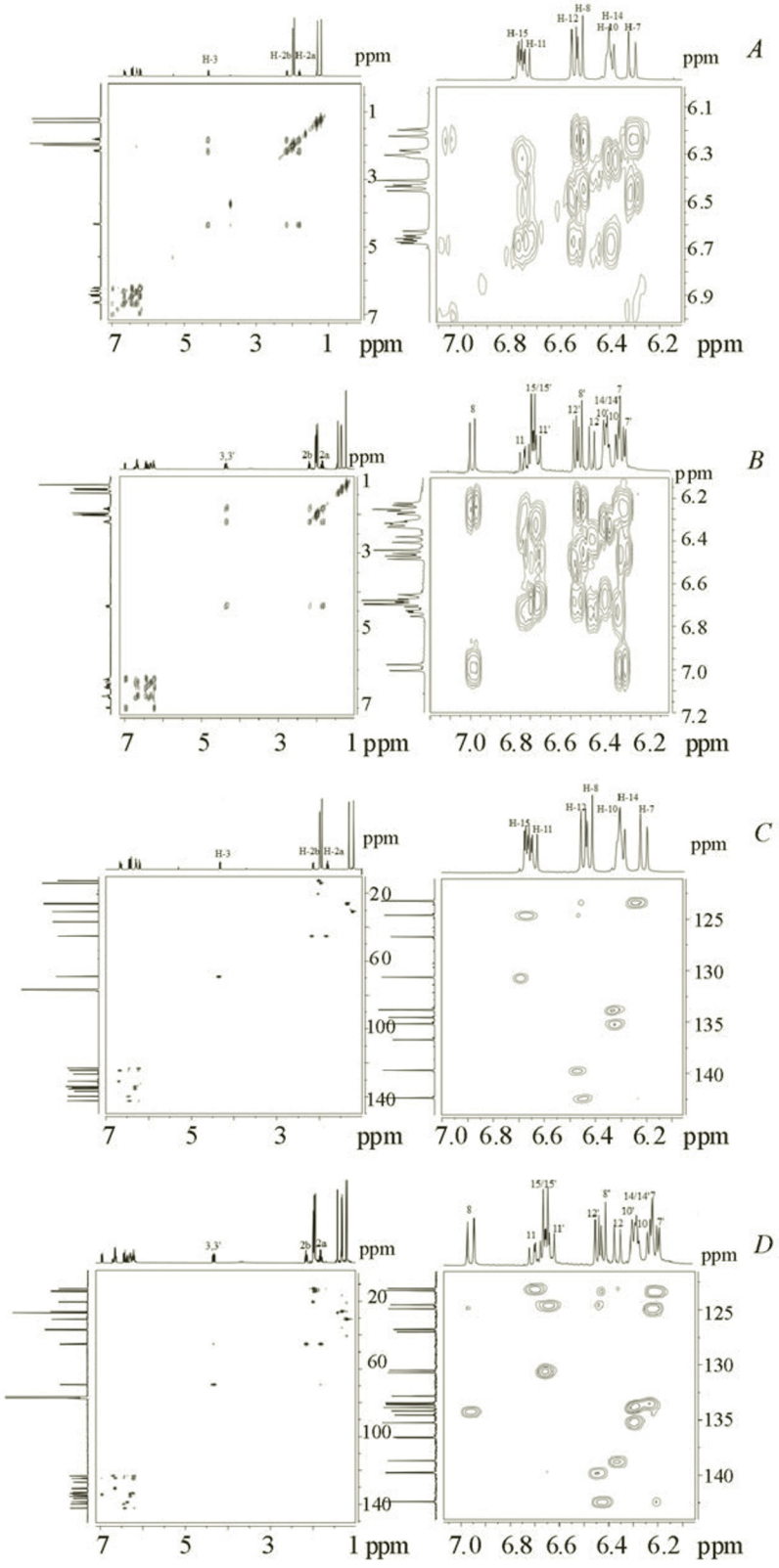

Fig. 6. Two-dimensional (2D) $^{1}H–^{1}H$ COSY (A, B) and $^{1}H–^{13}C$ HSQC (C, D) NMR spectra of all-*trans* (A, C) and 9-*cis* astaxanthin (B, D) in deuterated chloroform ($CDCl_3$); (a) full spectrum; (b) local amplification.

(HSQC) spectra is necessary. Once the assignment of proton signals is determined, all of the carbon signals in the ^{13}C NMR can be pointed out with the assistance of the HSQC spectrum, as the HSQC study provides the correlation between carbons and directly connected protons [32]. From the HSQC spectra, the alkyl carbons for all-*trans* or 9-*cis* can be determined easily, such as the carbon at 45.31 ppm (C-2/2′) of the 9-*cis* isomer individually associated with the protons at 1.82 (H-2/2′a) and 2.16 ppm (H-2/2′b). The most crucial factor is that the overlap districts H-14/14′/10′ and H-15/15′/11′ in the ^{1}H NMR can be distinguished according to the correlation between H-10′ (6.30 ppm) and C-10′ (133.82 ppm), as well as H-14/14′ (6.26–6.30 ppm) and C-14/14′ (133.40–135.22 ppm).

Conclusions. All-*trans*, 9-*cis*, 13-*cis*, and 15-*cis* astaxanthin were successfully isolated in gram-scale levels and verified with open column chromatography using silica gel columns and thin-layer chromatography. In turn, the purities and structures of astaxanthin were determined primarily using a combination of C_{30}-HPLC and Si_{60}-HPLC. Moreover, this is the first report on the complete identification of astaxanthin isomers, especially 9-*cis* by NMR, combined with FI-IR technology. We believe that the qualitative analytical methods included herein would be helpful for future applications such as confirmation of the purity and the elucidation of the structure of geometrical isomers of other carotenoids. Further studies are necessary to develop quantitative analytical methods to demonstrate the isomerization mechanism of astaxanthin and other carotenoids.

Acknowledgments. This work is funded by Natural Science Foundation of China (51703100), Ningbo Natural Science Foundation (2018A610098), and Zhejiang Public Welfare Fund (LGN18B060002).

REFERENCES

1. M. Guerin, M. E. Huntley, and M. Olaizola, *Trends Biotechnol.*, **21**, 210–216 (2003).
2. M. Cianci, P. J. Rizkallah, A. Olczak, J. Raftery, N. E. Chayen, P. F. Zagalsky, and J. R. Helliwell, *Proc. Nat. Acad. Sci. USA,* **99**, 9795–9800 (2002).
3. Y. M. Naguib, *J. Agric. Food Chem.*, **48**, 1150–1154 (2000).
4. G. Hussein, U. Sankawa, H. Goto, K. Matsumoto, and H. Watanabe, *J. Nat. Prod.*, **69**, 443–449 (2006).
5. N. Shimidzu, M. Goto, and W. Miki, *Fisheries Sci*., **62**, 134–137 (1996).
6. H. Jyonouchi, S. Sun, K. Iijima, and M. D. Gross, *Nutr. Cancer.*, **36**, 59–65 (2000).
7. H. Kurihara, H. Koda, S. Asami, Y. Kiso, and T. Tanaka, *Life Sci.*, **70**, 2509–2520 (2002).
8. L. Zhang and H. Wang, *Mar. Drugs*, **13**, 4310–4330 (2015).
9. R. G. Fassett and J. S. Coombes, *Mar. Drugs*, **9**, 447–465 (2011).
10. R. G. Fassett and J. S. Coombes, *Future Cardiol.*, **5**, 333–342 (2009).
11. H. Wu, H. Niu, A. Shao, C. Wu, B. Dixon, J. Zhang, S. Yang, and Y. Wang, *Mar. Drugs*, **13**, 5750–5766 (2015).
12. X. Liu and T. Osawa, *Biochem. Biophys. Res. Commun.*, **357**, 187–193 (2007).
13. B. Bjerkeng, M. Følling, S. Lagocki, T. Storebakken, J. J. Olli, and N. Alsted, *Aquaculture*, **157**, 63–82 (1997).
14. J. P. Yuan and F. Chen, *J. Agric. Food Chem.*, **47**, 3656–3660 (1999).
15. J. P. Yuan and F. Chen, *Food Chem.*, **73**, 131–137 (2001).
16. W. J. De Bruijn, Y. Weesepoel, J. P. Vincken, and H. Gruppen, *Food Chem.*, **194**, 1108–1115 (2016).
17. A. Mortensen and L. H. Skibsted, *J. Agric. Food Chem.*, **48**, 279–286 (2000).
18. C. S. Chen, S. H. Wu, Y. Y. Wu, J. M. Fang, and T. H. Wu, *Org. Lett.*, **9**, 2985–2988 (2007).
19. L. Zhao, F. Chen, G. Zhao, Z. Wang, X. Liao, and X. Hu, *J. Agric. Food Chem.*, **53**, 9620–9623 (2005).
20. G. Euglert and M. Vecchi, *Helv. Chim. Acta*, **63**, 1711–1718 (1980).
21. D. Qiu, W. L. Zhu, C. K. Tang, L. F. Shi, and H. Q. Gao, *Food Anal. Methods*, **7**, 597–605 (2014).
22. D. Qiu, Y. C. Wu, W. L. Zhu, H. Yin, and L. T. Yi, *J. Food Sci.*, **77**, C934–C940 (2012).
23. M. D. Grynbaum, P. Hentschel, K. Putzbach, J. Rehbein, M. Krucker, G. Nicholson, and K. Albert, *J. Sep. Sci.*, **28**, 1685–1693 (2005).
24. F. Miao, D. Lu, Y. Li, and M. Zeng, *Anal. Biochem.*, **352**, 176–181 (2006).
25. D. Qiu, Y. Bai, and Y. C. Shi, *Food Chem.*, **135**, 665–671 (2012).
26. K. Holtin, M. Kuehnle, J. Rehbein, P. Schuler, G. Nicholson, and K. Albert, *Anal. Bioanal. Chem*., **395**, 1613 (2009).
27. R. N. Rao, S. N. Alvi, B. N. Rao, and H. Group, *J. Chromatogr. A*, **1076**, 189–192 (2005).
28. W. Sun, H. Lin, Y. Zhai, L. Cao, K. Leng, and L. Xing, *Sep. Sci. Technol.*, **50**, 1377–1383 (2015).
29. G. Britton, S. Liaaen-Jensen, and H. Pfander, *Carotenoids*, Vol. 1B: *Spectroscopy*, Birkhäuser (1994).

30. R. J. Anderson, D. J. Bendell, and P. W. Groundwater, *Organic Spectroscopic Analysis*, Royal Soc. Chem. (2004).
31. K. Pihlaja and E. Kleinpeter, *Carbon-13 NMR Chemical Shifts in Structural and Stereochemical Analysis*, John Wiley and Sons (1994).
32. N. Kumar, S. R. Devineni, G. Singh, A. Kadirappa, S. K. Dubey, and P. Kumar, *J. Pharm. Biomed.*, **119**, 114–121 (2016).